

Article

Ionic Fracture Fluid Leak-Off

Vladimir Shelukhin ^{1,*} and Mikhail Epov ²

¹ Lavrentyev Institute of Hydrodynamics, Novosibirsk State University, Novosibirsk 630090, Russia

² Trofimuk Institute of Oil and Gas Geology and Geophysics, Novosibirsk State University, Novosibirsk 630090, Russia; EpovMI@ipgg.sbras.ru

* Correspondence: shelukhin@list.ru

Received: 10 January 2019; Accepted: 15 February 2019; Published: 19 February 2019



Abstract: The study is motivated by monitoring the space orientation of a hydrolic fracture used in oil production. Streaming potential arises due to the leakage of ionic fracking fluid under the rock elastic forces which make the fracture disclosure disappear after pumping stops. The vector of electric field correlates with the fracture space orientation since the fluid leakage is directed normally to the fracture surfaces. We develop a mathematical model for the numerical evaluation of the streaming potential magnitude. To this end, we perform an asymptotic analysis taking advantage of scale separation between the fracture disclosure and its length. The contrast between the virgin rock fluid and the fluid invading from the fracture is proved to be crucial in a build up of a net charge at the invasion front. Calculations reveal that an increase of the viscosity and resistivity contrast parameters results in an increase of the streaming potential magnitude. Such a conclusion agrees with laboratory experiments.

Keywords: ionic fluid flows in a porous medium; streaming potential; hydro-fracture

1. Introduction

In applying hydraulic fracturing treatment of rocks, one should prepare for execting the size of a fracture and its space orientation. One of the reasons is to avoid hydraulic connectivity of a production well with an injection one, since during water-flood of an initially oil-filled reservoir, encroaching water spoils hydrocarbon recovery. Directional fracturing is also of importance in petrothermal power production while designing geothermal circulation systems within the dry rocks [1]. Typical circulation systems consist of two wells connected by a fracture. By injecting water into the hot, deep, crystalline rocks, a huge amount of heat can be harnessed [2].

The pressure transient data during the injection fall-off test provide a way to determine the dimensions of an induced fracture but not its direction [3]. Microseismic measurements allow us to find the direction of the fracture [4]. However, the reliability of such measurements is not evident due to the extremely low energy of microseismic events and a high level of acoustic noise. Therefore, alternative approaches are of interest.

In this study, we estimate the electric field induced near the hydrofracture by leakage of a contrast fluid from the fracture under elastic forces in the rock which make the fracture disclosure disappear after pumping stops. The electric potential, known as the streaming potential, arises due to electrokinetic phenomena when ionic fluid moves through a porous rock [5]. The vector of the induced electric field is directed normally to the fracture surfaces, while the electric potential at the fracture surfaces strongly depends on the location of the invasion front of the fracture fluid. Polarization occurs due to charge concentration at the invasion front. The charge density can be evaluated via the resistivity jump across the front.

Streaming potential measurement is based on response (DC voltage) associated with the excess of electrical charge that is transported by flow of conductive fluids through porous media under a

pressure gradient or an electrical conductivity change. Such a method presents a key electrokinetic mechanism to study fluid flows in porous media. An electrical double layer (EDL) forms at the rock–fluid interfaces. The onset of fluid flow perturbs the distribution of the ions present in that layer and induces a current, which is the source of the streaming potential. This electrokinetic mechanism has been tested and employed in the laboratory to monitor the evolution of an oil–water encroachment front over time during hydrocarbon recovery. Earlier, the streaming potential dynamics were studied near the production well during water-flood of an initially oil-filled [6,7]. Calculations reveal [8] that encroaching water causes changes in the streaming potential at the production well which could be resolved above background electrical noise; water approaching the well could be detected at several 10s to 100s of meters away. The magnitude of the measured potential depends upon the production rate, the coupling between fluid and streaming potentials, and the nature of the front between the displaced oil and the displacing water. Similar results were obtained via simulation for the streaming potential near the injection borehole during drilling [9].

The fact that the induced electric field is orthogonal to the fracture surfaces allows one to tell the fracture direction starting from the electric field testing. If such a field can be strong enough, one can pass to the next step trying to invent a method of measuring the electric field close to the fracture. In this study, we do not address measurements.

In our mathematical approach, we take advantage of the scale difference between fracture disclosure and its length. With fracture disclosure being small, one can reduce fracture–rock interaction onto the central plane between the fracture surfaces. To evaluate the electric field near the fracture, we apply an asymptotic technique assuming that the contrast between the invasion zone and the virgin rock is small. Agreement with laboratory experiments on correlations between the variations of the streaming potential and fluid flow in the core-sample is provided [10]; it follows from our calculations that electric field in the core-sample can be increased in two ways: when the viscosity of the invading fluid decreases or when the electric conductivity of the invading fluid decreases. Thus, the proposed mathematical model explains the laboratory experiments [10] and set theoretical tools for the streaming potential method applied both in the tracking the water front during production operations and the hydro-fracture development.

2. Basic Equations

We treat the fluid-saturated rock as a Biot’s poroelastic medium enjoying quasi-static deformations and incompressible flows which are explained within mathematical models developed in [3,11]. According to this model, the fluid mass balance and the momentum law of the poroelastic medium are given by the equations

$$\frac{\partial(\rho_f \phi)}{\partial t} + \text{div}(\rho_f \mathbf{Q}) = 0, \quad 0 = \text{div} \tau + \mathbf{g}\rho. \tag{1}$$

Here,

$$\tau = (\lambda \text{div} \mathbf{u} - \alpha_* p) \cdot \mathbf{I} + 2\mu \mathcal{E}(u), \quad \rho = \phi \rho_f + (1 - \phi) \rho_s,$$

where ϕ is the porosity, \mathbf{Q} is the Darcy velocity, ρ_f is the fluid density, ρ_s is the solid density, τ is the effective stress tensor, p is the pore pressure, \mathcal{E} is the deformation tensor, \mathbf{u} is the rock displacement vector, α_* is the Biot number, \mathbf{g} is the gravitational acceleration vector, μ and λ are the elasticity moduli. We use the notations

$$(\text{div} \tau)_i = \frac{\partial \tau_{ij}}{\partial x_j}, \quad \text{div} \mathbf{u} = \frac{\partial u_j}{\partial x_j}, \quad \mathcal{E}_{ij} = \frac{1}{2} \left(\frac{\partial u_i}{\partial x_j} + \frac{\partial u_j}{\partial x_i} \right).$$

An equilibrium state before fracturing is described by the equations

$$0 = \text{div} \tau_* + \mathbf{g}\rho, \quad \tau_* = (\lambda \text{div} \mathbf{u}_* - \alpha_* p_*) \cdot \mathbf{I} + 2\mu \mathcal{E}(u_*). \tag{2}$$

Here, \mathbf{I} is the identity tensor, τ_* is the equilibrium stress tensor in the rock before fracturing, $p_\infty = \rho_f g h$ is the equilibrium pore pressure, \mathbf{u}_* is the equilibrium rock displacement. The equilibrium state is determined by regional stresses as follows. Let us consider a vertical cylinder of the thickness $2h_0$ which is in equilibrium state and which is compressed from above by a poroelastic medium of thickness h , $h_0 \ll h$. It is proved in [3] that vertical load is transmitted to horizontal compression by the formula

$$\mathbf{n} \cdot \tau_* \langle \mathbf{n} \rangle = -\lambda_l \sigma_h \equiv -\sigma_\infty,$$

where

$$\sigma_h = gh\rho, \quad \lambda_l = \frac{\nu}{1-\nu} + \frac{(1-2\nu)p_\infty\alpha_*}{\sigma_h(1-\nu)}, \quad (\tau \langle \mathbf{n} \rangle)_i = \tau_{ij}n_j,$$

\mathbf{n} is the unit external normal vector at the lateral cylinder surface, the point “ \cdot ” stands for the scalar product, ν is the Poisson coefficient, λ_l is the lateral stress coefficient.

Generally, porosity ϕ depends on pore pressure and rock compressibility, i.e., $\phi = \phi(p, J)$, $J = \text{tr}\mathcal{E}(\mathbf{u})$. By definition of the Biot number α_* , we have the equality $\partial\phi/\partial J = \alpha_*$ [12].

Let us introduce the compressibility coefficient $S = \partial\phi/\partial p$ and the deviation quantities

$$\mathbf{u}' = \mathbf{u} - \mathbf{u}_*, \quad p' = p - p_\infty, \quad \tau' = \tau - \tau_*.$$

Then Equation (1) become

$$\alpha_* \frac{\partial}{\partial t} \text{div } \mathbf{u}' + S p'_t + \text{div}(\rho_f \mathbf{Q}) = 0, \quad 0 = \text{div } \tau', \tag{3}$$

where

$$\tau' = (\lambda \text{div } \mathbf{u}' - \alpha_* p') \cdot \mathbf{I} + 2\mu \mathcal{E}(\mathbf{u}').$$

The fluid flux \mathbf{Q} obeys the generalized Darcy law which governs electrolyte flows in a porous medium [13–15]:

$$\mathbf{Q} = -\lambda_{11} \nabla p' - \lambda_{12} \nabla \psi, \quad \mathbf{J} = -\lambda_{21} \nabla p' - \lambda_{22} \nabla \psi, \quad \text{div } \mathbf{J} = 0, \tag{4}$$

where \mathbf{J} is the density of electric current, ψ is the streaming potential, λ_{ij} are electro-kinetic coefficients. It is the double electric layer (DEL) theory which lays behind the first two equations in (4). Particularly, these equations explain the electro-osmosis effect discovered by F.F. Reuss in 1808, Figure 1. The latter equation in (4) is known as the charge conservation law. By the two-scale homogenization theory, it is proved in [16] that λ_{ij} are given by the following representation formulas:

$$\lambda_{11} = \frac{k_r}{\eta_r}, \quad \lambda_{22} = \sigma_r, \quad \lambda_{12} = \lambda_{21} = F \sqrt{\lambda_{11} \lambda_{22}},$$

where k_r is the rock permeability, η_r is the dynamical viscosity of the pore fluid, σ_r is the effective density of the electric conductivity, F is the dimensionless tortuosity. For sandstones, $F \simeq 0.001$ [8,16].

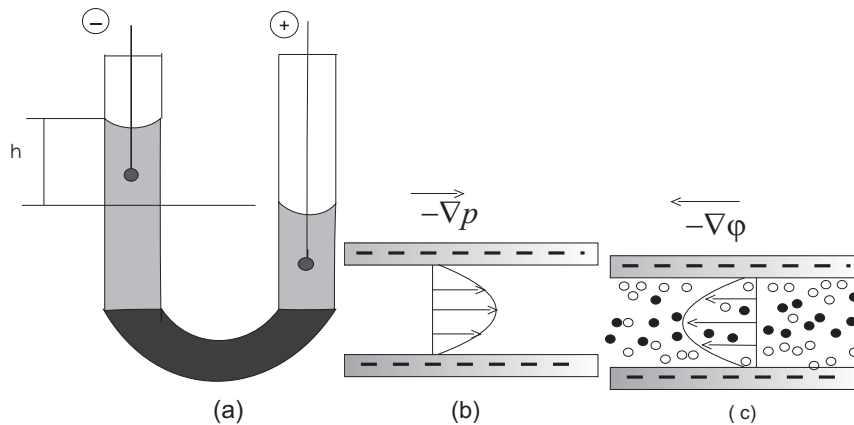


Figure 1. (a) F.F. Reuss experiment (1808) with water in the U-tube plugged with sandstone sample: applied electric field results in water level change of the height h (effect of electroosmos). (b) Pressure driven flow in a pore space. (c) Due to the double electric layer (DEL) theory, there is an excess of ions of the same sign in the bulk pore fluid. As a result, a flow occurs if an electric field is applied.

In [17,18], a mathematical model and a computer code are developed for calculation of the electric conductivity σ_r of a saturated rock. The model allows one to determine an optimal Archie-like law

$$\frac{\sigma_r}{\sigma_f} = s_*^q \left(\frac{\phi - \phi_p}{1 - \phi_p} \right)^m,$$

where σ_f is the density of the pore fluid electric conductivity, m is the cementation factor, s_* water saturation, q mineralization factor, and ϕ_p is the percolation limit.

We assume that a vertical fracture of height $2r$ and length $2R$ is extended along the horizontal x -axis and its disclosure along another horizontal y -axis does not depend on the vertical variable z , Figure 2a. We also assume that the fracture is symmetrical with respect to the y -axis, and the rock stress-strain state is symmetrical with respect to the x -axis and y -axis. Thus, in what follows we study a two-dimensional problem with all the vectors lying in the horizontal plane (x, y) .

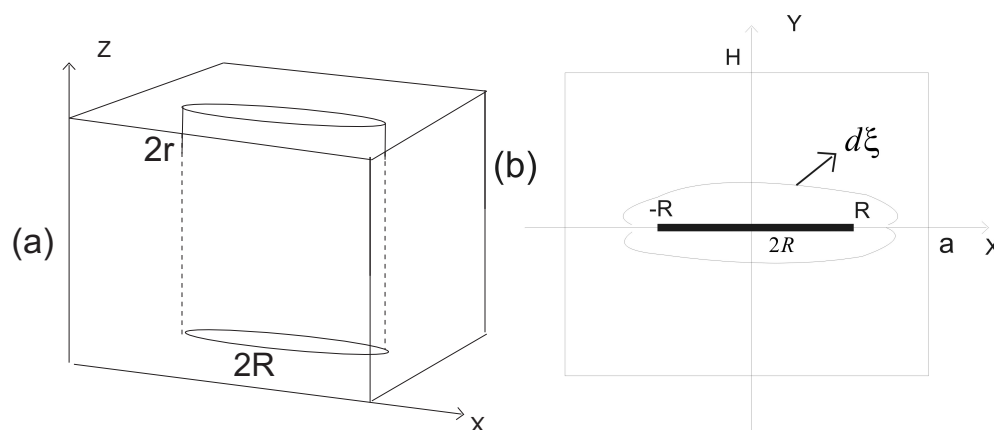


Figure 2. (a) Schematic of a hydrofracture with the height $2r$ and the length $2R$. (b) Schematic of an invasion front near the fracture when it is associated with its footprint interval $(-R, R)$.

Let us write the mass conservation law for fracture fluid. As in the lubrication theory, we have (Batchelor, 1967)

$$w_t + \frac{\partial}{\partial x}(wV) = -q.$$

Here, w stands for one-half the fracture aperture. By continuity of displacements,

$$w(x, t) = \mathbf{u}' \cdot \mathbf{e}_y|_{y=0}, \tag{5}$$

where \mathbf{e}_y is the unite vector along the y -axis, q is the fluid leakage, $V(t, x)$ is the fluid velocity along the x -axis. The velocity V enjoys the representation

$$V = -\frac{(2w)^2}{12\eta_c} p'_{x'}, \tag{6}$$

where η_c is the viscosity of the fracture fluid. It is remarked in [3] that one can use the following alternative formula:

$$V = -\frac{k_c}{\phi_c \eta_c} p'_{x'}, \tag{7}$$

where k_c is the fracture permeability and ϕ_c is the fracture porosity.

Leakage from the fracture satisfies the continuity condition

$$q = -(\lambda_{11} \nabla p - \lambda_{12} \nabla \psi) \cdot \mathbf{e}_y|_{y=0}. \tag{8}$$

It was proved in [19,20] that the invasion front can be determined by the method of characteristics from the following equation for the position vector $\xi = (\xi_1, \xi_2)$ at the (x, y) -plane:

$$\phi \frac{d}{dt} \xi = \mathbf{Q}(x, y, t)|_{x=\xi_1, y=\xi_2}. \tag{9}$$

It means that the infinitesimal displacement $d\xi$ of the front point (ξ_1, ξ_2) is equal to $\mathbf{Q}(\xi_1, \xi_2, t)dt/\phi$, Figure 2b.

Let us comment on the front since it plays a crucial role in the study. Mathematically, the front can be associated with the interface $F(x, y, t) = 0$, with $F(x, y, t)$ being a scalar function. It means that the solution $\xi(t)$ of (9) satisfies the equation $F(\xi(t), t) = 0$. Propagation of the interface F along the normal vector $\mathbf{n} = \nabla F/|\nabla F|$ can be determined from Equation (9) as follows:

$$\mathbf{n} \cdot \mathbf{Q} + \frac{F_t}{|\nabla F|} = 0.$$

Let us denote by $[f]_{\xi}$ the jump of the function $f(x, y)$ across the interface F along the normal vector \mathbf{n} at the point ξ :

$$[f]_{\xi} = \lim_{\delta \rightarrow 0} \{f(\xi + \delta \mathbf{n}) - f(\xi - \delta \mathbf{n})\}.$$

By continuity,

$$[p]_{\xi} = 0, \quad [\psi]_{\xi} = 0, \quad [\mathbf{J} \cdot \mathbf{n}]_{\xi} = 0, \quad [\mathbf{Q} \cdot \mathbf{n}]_{\xi} = 0.$$

On the other hand, $[\lambda_{ij}]_{\xi} \neq 0$. Hence, $[\nabla \psi \cdot \mathbf{n}]_{\xi} \neq 0$. The latter condition implies that there is a charge concentration at the interface F . In short, our goal is to determine dynamics of the jump $[\nabla \psi \cdot \mathbf{n}]_{\xi}$.

Let us formulate boundary-value conditions for the fracture lying in the rectangular

$$\Omega_1 = \{(x, y) : |x| < a, |y| < H\}.$$

Since the fracture aperture is small compared to its length we reduce fracture-rock interactions to its footprint, Figure 1b,

$$F_c = \{(x, y) : |x| < R, y = 0\}.$$

Because of symmetry we study flows and deformations in the half domain $\Omega_1^+ = \Omega_1 \cap \{y > 0\}$ only.

We assume that the pressure and stress at the external boundary $\partial\Omega_1 \cap (y > 0)$ coincide with the regional values. This is why in terms of deviated quantities we impose the following conditions:

$$\partial\Omega_1 : \quad \mathbf{n} \cdot \boldsymbol{\tau}' \langle \mathbf{n} \rangle = 0, \quad \mathbf{s} \cdot \boldsymbol{\tau}' \langle \mathbf{n} \rangle = 0, \quad p' = 0, \quad \psi = \psi_\infty, \quad (10)$$

where \mathbf{s} is the unite vector tangential to the boundary $\partial\Omega_1$, ψ_∞ is the prescribed streaming potential. Stress continuity at the rock–fracture interface reduces to the footprint F_c as follows

$$y = 0, |x| < L : \quad \mathbf{n} \cdot \boldsymbol{\tau}' \langle \mathbf{n} \rangle = \sigma_\infty - p_\infty - p', \quad \mathbf{s} \cdot \boldsymbol{\tau}' \langle \mathbf{n} \rangle = 0, \quad \psi = \psi_c, \quad (11)$$

where ψ_c is the streaming potential inside the fracture. Pressure continuity at the rock–fracture interface implies that the pore pressure and the fracture pressure coincide at $y = 0$. Outside the fracture, we impose the following symmetry conditions

$$\frac{\partial}{\partial y}(\mathbf{u}' \cdot \mathbf{e}_x) = 0, \quad \mathbf{u}' \cdot \mathbf{e}_y = 0, \quad \frac{\partial p'}{\partial y} = 0, \quad \frac{\partial \psi}{\partial y} = 0.$$

To complete the picture, one should set initial conditions. We shall do it in what follows.

3. Very Long Fracture

Our goal is determine correlations between streaming potential dynamics and invasion front propagation. To perform asymptotic analysis, we pass to a simplified problem under the following hypotheses. We assume that the fracture aperture is the same along the fracture, with the latter being infinite. In this case $a = L = \infty$ and the solution depends on time and the space variable y only, $0 < y < H$.

We denote

$$v(t, y) = \mathbf{u}' \cdot \mathbf{e}_y, \quad \xi = \xi_2.$$

Omitting the prime in the pressure notation p' , we arrive at the following equations for the functions v, p, ψ, ξ in the domain $0 < y < H$:

$$0 = \frac{\partial}{\partial y} [(\lambda + 2\mu)v_y - \alpha_* p], \quad (12)$$

$$\alpha_* v_{yt} + Sp_t = \frac{\partial}{\partial y} [\lambda_{11} p_y + \lambda_{12} \psi_y] \quad (13)$$

$$0 = \frac{\partial}{\partial y} [\lambda_{21} p_y + \lambda_{22} \psi_y] \quad (14)$$

$$\phi \xi_t = - [\lambda_{11} p_y + \lambda_{12} \psi_y] \Big|_{y=\xi}. \quad (15)$$

Boundary conditions become

$$y = 0 : \quad v_t = \lambda_{11} p_y + \lambda_{12} \psi_y, \quad (\lambda + 2\mu)v_y + (1 - \alpha_* p) = \sigma_\infty - p_\infty, \quad \psi = \psi_c, \quad (16)$$

$$y = H : (\lambda + 2\mu)v_y - \alpha_* p = 0, \quad p = 0, \quad \psi = \psi_\infty. \quad (17)$$

It is crucial in the present study that the kinetic coefficients λ_{ij} undergo jumps at the invasion front:

$$\lambda_{ij} = \begin{cases} \lambda_{ij}^-, & 0 < y < \xi(t), \\ \lambda_{ij}^+, & \xi(t) < y < H, \end{cases} \quad (18)$$

with λ_{ij}^- and λ_{ij}^+ being different constants.

Let us analyse system (12)–(17). Equation (12) implies that the function $\beta_1 \equiv (\lambda + 2\mu)v_y - \alpha_* p$ does not depend on the variable y . Now, it follows from the boundary condition (17) that $\beta_1 = 0$. Hence, one can exclude the function v by the formula

$$v_y = \frac{\alpha_*}{\lambda + 2\mu} p.$$

One can derive from (17) the following boundary condition for pressure at $y = 0$:

$$y = 0: \quad p = \sigma_\infty - p_\infty \tag{19}$$

By Equation (14), the function

$$\beta \equiv -\lambda_{21} p_y - \lambda_{22} \psi_y \tag{20}$$

does not depend on y . Clearly,

$$\psi_y = -\frac{\beta + \lambda_{21} p_y}{\lambda_{22}}. \tag{21}$$

We conclude from (16) and (21) that the fracture disclosure can be determined from the equation

$$y = 0: \quad v_t = \left(\lambda_{11} - \frac{\lambda_{12} \lambda_{21}}{\lambda_{22}} \right) p_y - \frac{\lambda_{12}}{\lambda_{22}} \beta. \tag{22}$$

Let us integrate equality (20) paying attention to jumps of λ_{ij} :

$$\begin{aligned} \beta \xi &= -\lambda_{21}^-(p|_\xi - p|_0) - \lambda_{22}^-(\psi|_\xi - \psi|_0), \\ \beta(H - \xi) &= -\lambda_{21}^+(p|_H - p|_\xi) - \lambda_{22}^+(\psi|_H - \psi|_\xi). \end{aligned}$$

By excluding $\psi|_\xi$, we find the following representation for $\beta(t)$:

$$\beta = \frac{n_1 + n_2 p|_\xi}{n_3 \xi(t) + n_4 (H - \xi(t))}, \quad p|_\xi \equiv p(t, y)|_{y=\xi(t)}, \tag{23}$$

where

$$n_1 = \psi_c - \psi_\infty + \frac{\lambda_{21}^-}{\lambda_{22}^-} (\sigma_\infty - p_\infty), \quad n_2 = \left[\frac{\lambda_{21}}{\lambda_{22}} \right]_\xi, \quad n_3 = \frac{1}{\lambda_{22}^-}, \quad n_4 = \frac{1}{\lambda_{22}^+}.$$

Here and in what follows, $[f]_\xi$ stands for jump of the function $f(y)$ at the point ξ :

$$[f]_\xi = f(\xi+) - f(\xi-) \equiv \lim_{\delta \rightarrow 0} (f(\xi + \delta) - f(\xi - \delta)).$$

Thus, by eliminating displacement and potential, we reduce the problem (12)–(17) to the following mathematical model. We look for unknown functions $p(t, y)$, $\xi(t)$, satisfying the equations:

$$\left(S + \frac{\alpha_*^2}{\lambda + 2\mu} \right) \frac{\partial p}{\partial t} + \frac{\partial Q}{\partial y} = 0, \quad Q \equiv -\frac{\Delta_\lambda}{\lambda_{22}} p_y + \frac{\lambda_{12}}{\lambda_{22}} \beta(t), \quad \Delta_\lambda \equiv \lambda_{11} \lambda_{22} - \lambda_{12} \lambda_{21}, \tag{24}$$

$$\phi \frac{d\xi}{dt} = Q(t, y)|_{y=\xi(t)-}, \tag{25}$$

$$p|_{y=0} = \sigma_\infty - p_\infty, \quad p|_{y=H} = 0. \tag{26}$$

Observe, that solution should obey the no-jump restrictions:

$$[p]_\xi = 0, \quad [Q]_\xi = 0.$$

Let us pass to dimensionless variables

$$z = \frac{y}{H}, \quad \bar{p} = \frac{p}{p_*}, \quad \tau = \frac{t}{T}, \quad \tilde{\psi} = \frac{\psi}{\psi_*}, \quad \zeta = \frac{\xi}{H}.$$

Now, the functions $\tilde{p}(\tau, z), \zeta(\tau)$ satisfy the equations

$$A_1 \tilde{p}_\tau = \frac{\partial}{\partial z} \left(A_2 \frac{\lambda_{11}}{\lambda_{11}^-} \tilde{p}_z - A_3 \tilde{\beta}(\tau) \frac{\lambda_{12} \lambda_{22}^-}{\lambda_{22} \lambda_{12}^-} \right), \quad \tilde{p}|_{z=0} = \frac{\sigma_\infty - p_\infty}{p_*}, \quad \tilde{p}|_{z=1} = 0, \tag{27}$$

$$\phi \zeta_\tau = A_6 \tilde{\beta}(\tau) - A_5 \tilde{p}_z|_{z=\zeta}, \tag{28}$$

on the dimensionless interval $0 < z < 1$. Here, A_i are dimensionless parameters:

$$A_1 = 1 + \frac{\alpha_*^2}{S(\lambda + 2\mu)}, \quad A_2 = \frac{T}{H^2 S} \frac{\Delta \lambda^-}{\lambda_{22}^-} = \frac{\lambda_{11}^- (1 - F^2) T}{H^2 S}, \quad A_3 = \frac{\psi_* T \lambda_{12}^-}{H^2 S p_*},$$

$$A_4 = \frac{p_* \lambda_{21}^-}{\psi_* \lambda_{22}^-}, \quad A_5 = \frac{p_* T}{H^2} \frac{\Delta \lambda^-}{\lambda_{22}^-} = \frac{p_* T \lambda_{11}^- (1 - F^2)}{H^2}, \quad A_6 = \frac{\psi_* T \lambda_{12}^-}{H^2}.$$

The kinetic coefficients λ_{ij} are stepwise functions:

$$\lambda_{ij} = \begin{cases} \lambda_{ij}^-, & 0 < z < \zeta(\tau), \\ \lambda_{ij}^+, & \zeta(\tau) < z < 1. \end{cases}$$

We denote

$$\Delta \tilde{\psi} = \tilde{\psi}|_{z=1} - \tilde{\psi}|_{z=0}, \quad \Delta \tilde{p} = \tilde{p}|_{z=1} - \tilde{p}|_{z=0}.$$

The function $\tilde{\beta}(\tau)$ is given by the formula

$$\tilde{\beta} = \frac{-\Delta \tilde{\psi} - A_4 \Delta \tilde{p} + \tilde{p}(\zeta(\tau), \tau) A_4 \left\{ \lambda_{21}^+ \lambda_{22}^- / (\lambda_{21}^- \lambda_{22}^+) - 1 \right\}}{\zeta + (1 - \zeta) \lambda_{22}^- / \lambda_{22}^+}.$$

By definition, $\tilde{\beta}$ is dimensionless electric current density since $\tilde{\beta} = \frac{\beta H}{\psi_* \lambda_{22}^-}$ and $\beta \equiv J$ is dimension electric current density.

We formulate initial conditions as follows:

$$\tilde{p}|_{\tau=0} = \tilde{p}_0(z), \quad \zeta|_{\tau=0} = 0. \tag{29}$$

Choosing $p_* = \sigma_\infty - p_\infty$, we obtain that $\tilde{p}|_{z=0} = 1$ and $\Delta \tilde{p} = -1$. Observe that we study electric field induced by the fracture closing. Hence, initial fracture aperture is assumed known and it will appear in what follows.

The solution obeys the following no-jump restrictions:

$$[\tilde{p}]_\zeta = 0, \quad \left[A_2 \frac{\lambda_{11}}{\lambda_{11}^-} \tilde{p}_z \right]_\zeta = \tilde{\beta}(\tau) A_3 \left[\frac{\lambda_{12} / \lambda_{12}^-}{\lambda_{22} / \lambda_{22}^-} \right]_\zeta. \tag{30}$$

Given the functions $\tilde{p}(z, \tau)$ and $\zeta(\tau)$, one can determine dimensionless electric field by the formula

$$E' = -\tilde{\psi}_z = \frac{\tilde{\beta} + (\lambda_{12} / \lambda_{12}^-) A_4 \tilde{p}_z}{\lambda_{22} / \lambda_{22}^-}. \tag{31}$$

4. Asymptotic Analysis

Observe, that (27) is not a differential equation in the common sense since it contains not only partial derivatives of $\tilde{p}(z, \tau)$ at the running point (z, τ) but at the point $(\zeta(\tau), \tau)$ also, with $\zeta(\tau)$ being unknown function. It is the main mathematical difficulty of the study. Up to now, no tools are developed to solve the problem numerically. This is why we try to solve it analitically applying an asymptotic analysis. There are publications on differential equations which contain partial derivatives at the running point (z, τ) and a point (z_0, τ) , with z_0 being fixed. Such equations are known as loaded differential equations.

We analyse system (27)–(29) under the assumption that jumps of the coefficients λ_{ij} are small in the sense that there is a small ε such that $\lambda_{ij} = k_{ij}\varepsilon$ where the step-wise functions k_{ij} do not depend on ε . We perform an asymptotic analysis assuming that $\varepsilon \rightarrow 0$. Clearly, both the functions $\tilde{p}(\tau, z)$ and $\zeta(\tau)$ depend on ε . But there is a difficulty in addressing the difference $\tilde{p}^{\varepsilon_1}(\tau, z) - \tilde{p}^{\varepsilon_2}(\tau, z)$ starting from Equation (27) for $\tilde{p}^\varepsilon(\tau, z)$. The problem is that the coefficients λ_{ij} depend on ε also and undergo jumps across the moving unknown line $z = \zeta^\varepsilon(\tau)$. To emphasize that the functions λ_{ij} depend on ε , we write $\lambda_{ij}^\varepsilon(x, \tau)$ instead of $\lambda_{ij}(x, \tau)$.

The way to avoid this difficulty is to pass to new variables (x, τ) such that all the coefficients $\lambda_{ij}^\varepsilon(x, \tau)$ are defined on the same fixed domain. We define the change of variables $(z, \tau) \rightarrow (x, \tau)$ as follows:

$$x = \begin{cases} \frac{z-\zeta(\tau)}{1-\zeta(\tau)}, & \zeta(\tau) < z < 1, \\ \frac{z-\zeta(\tau)}{\zeta(\tau)}, & 0 < z < \zeta(\tau). \end{cases} \tag{32}$$

In new variables, the function $\tilde{p}^\varepsilon(x, \tau)$ is defined on the fixed interval $-1 < x < 1$ and the functions $\tilde{p}^\varepsilon(x, \tau), \zeta^\varepsilon(\tau)$ satisfy the equations

$$\begin{aligned} A_1 (\tilde{p}_t^\varepsilon + x_\tau \tilde{p}_x^\varepsilon) &= x_z \frac{\partial}{\partial x} \{ A_2 x_z a_1(x) \tilde{p}_x^\varepsilon - A_3 \tilde{\beta}(\tau) a_2(x) \}, \\ \tilde{p}^\varepsilon|_{x=-1} &= 1, \quad \tilde{p}^\varepsilon|_{x=1} = 0, \\ \phi \zeta_\tau^\varepsilon &= A_6 \tilde{\beta}(\tau) - \frac{A_5}{\zeta^\varepsilon} \tilde{p}_x^\varepsilon|_{x=0-}, \end{aligned}$$

where

$$\tilde{\beta} = \frac{-\Delta\tilde{\psi} - A_4\Delta\tilde{p}^\varepsilon + \tilde{p}^\varepsilon(0, \tau)A_4[a_2]_0}{\zeta^\varepsilon + (1 - \zeta)a_3}.$$

The functions $a_i(x)$ are defined in Appendix A.

The no-jump conditions at $x = 0$ become

$$x = 0 : \quad [\tilde{p}^\varepsilon]_0 = 0, \quad [A_2 a_1(x) x_z \tilde{p}_x^\varepsilon]_0 = \tilde{\beta}(\tau) A_3 [a_2(x)]_0.$$

We look for $\tilde{p}^\varepsilon(x, \tau), \zeta^\varepsilon(\tau)$ via the expansion series

$$\tilde{p}(x, \tau) = p^0(x, \tau) + \varepsilon p^1(x, \tau) + \dots, \quad \zeta(\tau) = \zeta^0(\tau) + \varepsilon \zeta^1(\tau) + \dots.$$

We prove in Appendix A, that the function $p^0(z, \tau)$ in the dimensionless physical variables is given by the formula

$$p^0 = 1 - z - \frac{\gamma}{\pi} e^{-A_2 \pi^2 \tau / A_1} \sin \pi z. \tag{33}$$

We derive from (A1) and (A2) that the function $\zeta^0(\tau)$ can be determine by the Cauchy problem

$$\phi \frac{d\zeta^0}{d\tau} = A_6 \beta^0 + A_5 \left[1 + \gamma e^{-A_2 \pi^2 \tau / A_1} \cos(\pi \zeta^0) \right], \quad \zeta^0|_{\tau=0} = 0.$$

Clearly, $\zeta^0(\tau)$ increases in time even if $\Delta\tilde{\psi} = 0$.

Let us determine approximate dimensionless electric current $\beta_a(\tau) = \beta^0 + \varepsilon\beta^1$, making use the formulas

$$\varepsilon \frac{k_{ij}}{\lambda_{ij}^-} = \frac{\lambda_{ij}^+ - \lambda_{ij}^-}{\lambda_{ij}^-}, \quad \varepsilon a_3^1 = 1 - \frac{\lambda_{22}^+}{\lambda_{22}^-},$$

$$p^0|_{x=0} = p^0|_{z=\zeta^0} = 1 - \zeta^0 - \frac{\gamma}{\pi} e^{-A_2 \pi^2 \tau / A_1} \sin \pi \zeta^0.$$

We find that

$$\beta_a(\tau) = -\Delta\tilde{\psi} + A_4 - A_4(1 - \zeta^0) \left(1 - \frac{\lambda_{12}^+}{\lambda_{12}^-}\right) + (1 - \zeta^0) \left(1 - \frac{\lambda_{22}^+}{\lambda_{22}^-}\right) \Delta\tilde{\psi}$$

$$- \gamma A_4 \left(\frac{\lambda_{12}^+}{\lambda_{12}^-} - \frac{\lambda_{22}^+}{\lambda_{22}^-}\right) \frac{\sin \pi \zeta^0}{\pi} e^{-A_2 \pi^2 \tau / A_1}.$$

In dimension variables the density of the electric current is given by the formula $J_a = \beta_a \psi_* \lambda_{22}^- / H$ [$\text{Vm}^{-1}\text{s}^{-1}$].

Starting from the definition (31), we calculate dimensionless gradient of potential using the formula

$$-\Psi_z(z, \tau) = \frac{\beta_a(\tau) + (\lambda_{12}(z, \tau) / \lambda_{12}^-) A_4 p_z^0(z, \tau)}{\lambda_{22}(z, \tau) / \lambda_{22}^-}. \tag{34}$$

Let us introduce the contrast parameters

$$a = \sqrt{\frac{\lambda_{11}^+}{\lambda_{11}^-}}, \quad b = \sqrt{\frac{\lambda_{22}^+}{\lambda_{22}^-}}.$$

When $\Delta\tilde{\psi} = 0$, it follows from (34) that

$$\Psi_z(z, \tau) = -A_4(1 - ab) \frac{[1 + \text{sign}(z - \zeta^0(\tau))] / 2 - (1 - \zeta^0(\tau))}{1 + (b^2 - 1)[1 + \text{sign}(z - \zeta^0(\tau))] / 2} + F(z, \tau) e^{-A_2 \pi^2 \tau / A_1}, \tag{35}$$

where

$$F(z, \tau) = \gamma A_4 \frac{\pi^{-1}(ab + b) \sin(\pi \zeta^0(\tau)) + \cos(\pi z)}{1 + (b^2 - 1)[1 + \text{sign}(z - \zeta^0(\tau))] / 2}.$$

We calculated dynamics of Ψ_z neglecting the second term in (35) which decreases exponentially in time. Figure 3 depicts the reduced potential gradient $\Psi_Z(z, \tau) \equiv \Psi_z / A_4$ across the invasion front $z = \zeta^0(\tau)$ for the case $a = 0.33$ and different values of b . Potential gradient jump implies charge concentration at the invasion front $z = \zeta^0(\tau)$. The charge concentration is build up as b grows. Observe that the signs of Ψ_z are different before and after the front.

Let us calculate $\Psi_z|_{\tau=0}$ within the fracture assuming that $\Delta\tilde{\psi} = 0$. We have

$$\Psi_z|_{z=0, \tau=0} = A_4 \left(1 - \frac{\lambda_{12}^+}{\lambda_{12}^-}\right) + \gamma A_4$$

Due to the formula, $\lambda_{12} = \lambda_{21} = F \sqrt{\lambda_{11} \lambda_{22}}$, we derive that

$$\Psi_z|_{z=0, \tau=0} = \frac{b p_* F}{a \psi_*} \sqrt{\frac{\lambda_{11}^+}{\lambda_{12}^-}} (1 - ab + \gamma) \tag{36}$$

Let us estimate magnitude of $\Psi_z|_{z=0,\tau=0}$ for the typical values of data given in Nomenclature setting $\gamma = 0$ for simplicity. In this case, $b^2 = 10^{-4}/6$. Thus, the dimension initial value of the electric field within the fracture is equal to

$$\frac{\psi^*}{H} \Psi_z|_{z=0,\tau=0} = 4.53 \cdot 10^{-4} \text{ V/m}.$$

It follows from (36), that electric field in the fracture can be increased in two ways: when the viscosity of the invasion fluid decreases or when the electric conductivity of the invasion fluid decreases. This conclusion agrees with the recent laboratory experiments [10].

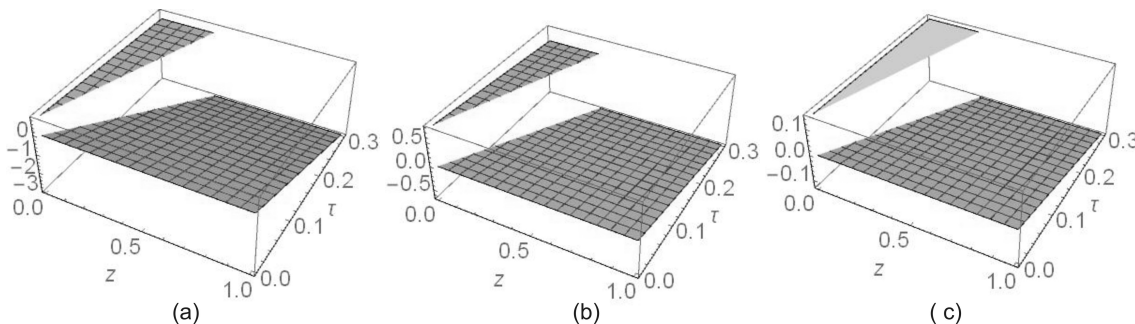


Figure 3. Reduced potential gradient $\Psi_Z(z, \tau) \equiv \Psi_z/A_4$ suffers a jump across the invasion front $z = \zeta^0(\tau)$. The contrast parameters are $a = 0.33$ and $b = 0.3, 0.6$ and 1.2 in (a–c) respectively.

5. Attenuation Time

The induced electric field exists until the fracture aperture disappears. To estimate the closure time, we introduce one more dimensionless parameter $A_7 = L/H$, where L is the one-half the initial fracture aperture. Let $\tilde{v}(\tau) = v/L$ stand for dimensionless fracture aperture at the dimensionless moment τ . Due to (22), $\tilde{v}(\tau)$ can be determined from the equation

$$x = -1 : A_7 \tilde{v}_\tau = A_5 \tilde{p}_x x_z - A_6 \tilde{\beta}, \quad \tilde{v}|_{\tau=0} = \tilde{v}_0.$$

We remind that $L\tilde{v}_0 = d_0 [sm]$ is the dimension initial fracture disclosure. A closure time τ_c satisfies the equality

$$-A_7 \tilde{v}_0 = \int_0^{\tau_c} (A_5 \tilde{p}_x x_z|_{x=-1} - A_6 \tilde{\beta}) d\tau.$$

Hence, approximately

$$-A_7 \tilde{v}_0 = \int_0^{\tau_c} (A_5 p_x^0 x_z^0|_{x=-1} - A_6 \beta^0) d\tau.$$

With the initial data given by (A2), the above equation is equivalent to

$$\tau_c \frac{A_5 + A_4 A_6 - \Delta \tilde{\psi} A_6}{A_7} - \tilde{v}_0 = -\frac{\gamma A_5}{A_7} \cdot \frac{1 - e^{-A_2 \pi^2 \tau_c / A_1}}{A_2 \pi^2 / A_1}.$$

Assuming that $\Delta \tilde{\psi} = 0$ and using the formula $e^{-x} \simeq 1 - x$, we derive that

$$\tau_c = \frac{A_7 \tilde{v}_0}{A_5 A_4 + A_6 + \gamma A_5}.$$

The dimension closure time is equal to

$$T\tau_c = \frac{d_0 H \eta_r^-}{p_* k_r^-} \cdot \frac{1}{1 + \gamma(1 - F^2)} \equiv \frac{d_0 H a^2}{p_* \lambda_{11}^+} \cdot \frac{1}{1 + \gamma(1 - F^2)}, \quad p_* = \sigma_\infty - p_\infty.$$

Setting $\gamma \simeq 1/2$ and applying the typical conditions given in Nomenclature, we find that the dimension closure time is equal to $T\tau_c \simeq 2$ [h], provided $d_0 = 0.5$ [sm]. One more conclusion is that the closure time decreases as the viscosity of fracture fluid decreases also.

6. Discussions and Conclusions

We formulated a mathematical model to evaluate the streaming potential induced by ionic fracture fluid leak-off after shut-in of a water injection well. Such a potential appears due to electro-kinetic effects relevant to electrolyte flows in a porous medium. The contrast between the virgin fluid and the fluid invading from the fracture is proved to be crucial in a build up of net charge at the invasion front. Calculations reveal that increase of the viscosity and resistivity contrasts results in increase of the streaming potential magnitude. To derive basic equations, we used the scale separation between the fracture disclosure and length. We developed an asymptotic series approach starting from the assumption the contrast parameters is small. The study is motivated by the observation that the vector of electric field correlates with the fracture space orientation since it is directed normally to the fracture surfaces.

Author Contributions: Conceptualization, V.S. and M.E.; methodology, V.S. and M.E.; software, V.S.; validation, V.S. and M.E.; formal analysis, V.S.; investigation, V.S. and M.E.; resources, M.E.; data curation, M.E; visualization, V.S.; supervision, M.E.; funding acquisition, M.E.

Funding: The research is partially supported by Grant of Government of Russian Federation No 14.W03.31.0002

Conflicts of Interest: The authors declare no conflict of interest.

Abbreviations

The following notations are used in this manuscript:

α_*	Biot's number, dimensionless, 0.7
μ	shear elasticity modulus, 8.95 [GPa], 1 [GPa] = $10 \left[\frac{\text{g}}{\text{cm} \cdot \text{s}^2} \right]$
λ	bulk elasticity modulus, $\lambda = 0.5 \mu$, [GPa]
ν	Poisson ratio, dimensionless, 0.25
ρ_f	fluid density, $1000 \left[\frac{\text{kg}}{\text{m}^3} \right]$
ρ_s	solid density, $2500 \left[\frac{\text{kg}}{\text{m}^3} \right]$
ϕ	porosity, dimensionless, 0.2
ρ	total density, $\rho = \phi \rho_f + (1 - \phi) \rho_s$, $\left[\frac{\text{kg}}{\text{m}^3} \right]$
g	gravitational acceleration, $980 \left[\frac{\text{cm}}{\text{s}^2} \right]$
S	compressibility, $S^{-1} = 0.0687$ [GPa]
H	domain's size of the nearby zone, 10 [m]
L	one-half the initial fracture aperture, 0.5 [cm]
T	characteristic time, 3600 [s]
ψ_*	reference value of streaming potential, 0.1 [mV], $1 [V^2] = 299.79^{-2} \left[\frac{\text{g} \cdot \text{cm}}{\text{s}^2} \right]$
h	depth, 2500 [m]
σ_h	rock's weight, $\sigma_h = \rho h g$, [GPa]
λ_l	lateral stress coefficient, dimensionless
σ_∞	regional stress, $\sigma_\infty = \lambda_l \sigma_h$, [GPa]
p_*	reference pressure, $p_* = \sigma_\infty - p_\infty$, [GPa]
k_r	rock permeability, 1 [mD], 1 [mD] = $0.987 \cdot 10^{-11}$ [cm ²]

- η_r^- dynamic viscosity of invasion fluid, 0.33 [cp], 1 [cp] = $10^{-2} \left[\frac{\text{g}}{\text{cm}\cdot\text{s}^2} \right]$
- η_r^+ dynamic viscosity of pore fluid, 3 [cp]
- σ_f^- specific electric conductivity of invasion fluid, $0.6 \left[\frac{\text{S}}{\text{m}} \right]$, $1 \left[\frac{\text{S}}{\text{m}} \right] = 9 \cdot 10^9 \left[\frac{1}{\text{s}} \right]$
- σ_f^+ specific electric conductivity of pore fluid, $10^{-5} \left[\frac{\text{S}}{\text{m}} \right]$
- s_* water saturation, dimensionless, $s_*^- = 0.7$, $s_*^+ = 0.1$
- m cementation factor, dimensionless, $m^- = 2$, $m^+ = 3$
- Φ_p percolation porosity limit, dimensionless, $\Phi_p^- = 0.008$, $\Phi_p^+ = 0.003$
- σ_r effective electric conductivity of saturated rock, $\left[\frac{\text{S}}{\text{m}} \right]$,
- $\sigma_r = s_*^q \sigma_f (\Phi - \Phi_p)^m$, $q = 2$
- F tortuosity, dimensionless, 10^{-3}
- λ_{ij} electrokinetic coefficients
- λ_{ij}^- electrokinetic coefficients in invasion zone
- λ_{ij}^+ electrokinetic coefficients in virgin zone
- $\lambda_{11} = k_r / \eta_r$
- $\lambda_{22} = \sigma_r$
- $\lambda_{12} = \lambda_{21} = F \sqrt{\lambda_{11} \lambda_{22}}$
- $A_1 = 1 + \frac{\alpha_*^2}{S(\lambda+2\mu)}$, dimensionless
- $A_2 = \frac{T}{H^2 S} \frac{\lambda_{11}^- \lambda_{22}^- - \lambda_{12}^- \lambda_{21}^-}{\lambda_{22}^-} = \frac{\lambda_{11}^- (1-F^2) T}{H^2 S}$, dimensionless
- $A_3 = \frac{\psi_* T \lambda_{12}^-}{H^2 S p_*}$, dimensionless
- $A_4 = \frac{p_* \lambda_{21}^-}{\psi_* \lambda_{22}^-}$, dimensionless
- $A_5 = \frac{p_* T}{H^2} \frac{\lambda_{11}^- \lambda_{22}^- - \lambda_{12}^- \lambda_{21}^-}{\lambda_{22}^-} = \frac{p_* T \lambda_{11}^- (1-F^2)}{H^2}$, dimensionless
- $A_6 = \frac{\psi_* T \lambda_{12}^-}{H^2}$, dimensionless
- $A_7 = \frac{L}{H}$, dimensionless

Appendix A

It follows from (32) that

$$x_z = \begin{cases} \frac{1}{1-\zeta(\tau)}, & 0 < x < 1, \\ \frac{1}{\zeta(\tau)}, & -1 < x < 0, \end{cases} \quad x_\tau = \begin{cases} \frac{\zeta_\tau(\tau)(x-1)}{1-\zeta(\tau)}, & 0 < x < 1, \\ -\frac{\zeta_\tau(\tau)(1+x)}{\zeta(\tau)}, & -1 < x < 0. \end{cases}$$

Let us introduce the functions

$$a_1(x) = \begin{cases} \lambda_{11}^+ / \lambda_{11}^-, & 0 < x < 1, \\ 1, & -1 < x < 0, \end{cases}$$

$$a_2(x) = \begin{cases} \lambda_{12}^+ \lambda_{22}^- / (\lambda_{12}^- \lambda_{22}^+), & 0 < x < 1, \\ 1, & -1 < x < 0, \end{cases}$$

and denote $a_3 = \lambda_{22}^- / \lambda_{22}^+$. Observe that the parameter a_3 and the functions $a_i(x)$, $\tilde{\beta}(\tau)$, $x(z, \tau)$ depend on ε .

Let us write expansion series for $a_i(x)$:

$$a_i = a_i^0 + \varepsilon a_i^1 + \dots$$

Starting from the definition of the functions $a_i(x)$, we find that $a_i^0 = 1$, $a_3^1 = -k_{22} / \lambda_{22}^-$, and

$$a_1^1 = \begin{cases} k_{11} / \lambda_{11}^-, & 0 < x < 1, \\ 0, & -1 < x < 0, \end{cases} \quad a_2^1 = \begin{cases} k_{12} / \lambda_{12}^- - k_{22} / \lambda_{22}^-, & 0 < x < 1, \\ 0, & -1 < x < 0, \end{cases}$$

Similarly, we find that

$$x_z(x, \tau) = x_y^0(x, \tau) + \epsilon x_z^1(x, \tau) + \dots, \quad x_\tau(x, \tau) = x_\tau^0(x, \tau) + \epsilon x_\tau^1(x, \tau) + \dots,$$

where

$$\begin{aligned} x_z^0 &= \begin{cases} (1 - \zeta^0)^{-1}, & 0 < x < 1, \\ 1/\zeta^0, & -1 < x < 0, \end{cases} \\ x_\tau^0 &= \begin{cases} \zeta_\tau^0(x - 1)/(1 - \zeta^0), & 0 < x < 1, \\ -\zeta_\tau^0(1 + x)/\zeta^0, & -1 < x < 0, \end{cases} \\ x_z^1 &= \begin{cases} \zeta^1/(1 - \zeta^0)^{-2}, & 0 < x < 1, \\ -\zeta^1/(\zeta^0)^2, & -1 < x < 0, \end{cases} \\ x_\tau^1 &= \begin{cases} [\zeta_\tau^1(x - 1)(1 - \zeta^0) + \zeta_\tau^0(x - 1)\zeta^1]/(1 - \zeta^0)^{-2}, & 0 < x < 1, \\ (-\zeta_\tau^1(1 + x)\zeta^0 + \zeta_\tau^0(1 + x)\zeta^1)/(\zeta^0)^2, & -1 < x < 0, \end{cases} \end{aligned}$$

Writing the expansion series

$$\tilde{\beta}(\tau) = \beta^0(\tau) + \epsilon\beta^1(\tau) + \dots,$$

one can derive that

$$\beta^0 = -\Delta\tilde{\psi} + A_4, \quad \beta^1 = A_4[a_2^1]_0 p^0(0, \tau) - \beta^0(1 - \zeta^0)a_3^1.$$

Setting the expansion series for a_i , $x(z, \tau)$ and $\tilde{\beta}(\tau)$ in Equations (27) and (28), we find that the functions $p^0(x, \tau)$, $\zeta^0(\tau)$ can be determine from the equations

$$\begin{aligned} A_1 a_4^0(x) p_\tau^0 - A_2 p_{xx}^0 - A_1 a_5^0(x) p_x^0 &= 0, \quad x \neq 0, \\ p^0|_{x=-1} = 1, \quad p^0|_{x=1} &= 0, \\ [p^0]_0 = 0, \quad [x_z^0 p_x^0]_0 = 0, \quad \phi \zeta_\tau^0 &= A_6 \beta^0 - A_5 p_x^0|_{x=0-}/\zeta^0, \end{aligned}$$

where

$$a_4 = \begin{cases} (1 - \zeta^0)^2, & 0 < x < 1, \\ (\zeta^0)^2, & -1 < x < 0, \end{cases} \quad a_5 = \begin{cases} (x - 1) ((1 - \zeta^0)^2)_\tau / 2, & 0 < x < 1, \\ (1 + x) ((\zeta^0)^2)_\tau / 2, & -1 < x < 0. \end{cases}$$

Similarly, we find that the functions $p^1(x, \tau)$ and $\zeta^1(\tau)$ can be determine from the equations

$$\begin{aligned} A_1 a_4^0(x) p_\tau^1 - A_2 p_{xx}^1 - A_1 a_5^0(x) p_x^1 &= a_6^0 p_\tau^0 + a_7^0 p_x^0 + a_8^0 p_{xx}^0, \quad x \neq 0, \\ p^0|_{x=-1} = 0, \quad p^0|_{x=1} = 0, \quad [p^1]_0 &= 0, \\ [A_2(x_z^1 p_x^0 + x_z^0 a_1^1 p_x^0 + x_z^0 p_x^1)]_0 &= [A_3 \beta^0 a_2^1]_0, \\ \phi \zeta_\tau^1 &= A_6 \beta^1 - A_5 \frac{p_x^1 \zeta^0 - p_x^0 \zeta^1}{(\zeta^0)^2}|_{x=0-}, \end{aligned}$$

where $a_8 = A_2 a_1^1$ and

$$\begin{aligned} a_6 &= \begin{cases} 2A_1(1 - \zeta^0)\zeta^1, & 0 < x < 1, \\ -2A_1\zeta^0\zeta^1, & -1 < x < 0, \end{cases} \\ a_7 &= \begin{cases} -A_1((1 - \zeta^0)\zeta^1)_\tau(x - 1), & 0 < x < 1, \\ A_1(\zeta^0\zeta^1)_\tau(1 + x), & -1 < x < 0. \end{cases} \end{aligned}$$

Let us return to the physical dimensionless variables (z, τ) , substituting $\zeta(\tau)$ in (32) by $\zeta^0(\tau)$. In the variables (z, τ) , the functions $p^0(z, \tau)$ and $\zeta^0(\tau)$ satisfy the equations

$$0 < z < 1: \quad A_1 p_\tau^0 = A_2 p_{zz}^0, \quad p^0|_{z=0} = 1, \quad p^0|_{z=1} = 0,$$

$$\phi \frac{d\zeta^0}{d\tau} = A_6 \beta^0 - A_5 p_z^0|_{z=\zeta^0}, \quad \zeta_0|_{\tau=0} = 0. \quad (\text{A1})$$

To evaluate the electric field, we choose the initial data in (29) as follows

$$\tilde{p}|_{\tau=0} = 1 - z - \frac{\gamma}{\pi} \sin \pi z, \quad (\text{A2})$$

where $0 \leq \gamma \leq 1$. Under such an assumption, we arrive at Formula (33).

References

1. Ziagos, J.; Phillips, B.R.; Boyd, L.; Jelacic, A.; Stillman, G.; Hass, E. Technology roadmap for strategic development of enhanced geothermal systems. In Proceedings of the 38-th Workshop on Geothermal Reservoir Engineering, Stanford University, Stanford, CA, USA, 11–13 February 2013; SGP-TR-198.
2. Hunsbedt, A.; Kruger, P.; London, A.L. Energy Extraction from a Laboratory Model Fractured Geothermal Reservoir. *J. Petrol. Technol.* **1978**, *30*, 712–718. [[CrossRef](#)]
3. Shelukhin, V.V.; Baikov, V.A.; Golovin, S.V.; Davletbaev, A.Y.; Starovoirov, V.N. Fractured water injection wells: Pressure transient analysis. *Int. J. Solids Struct.* **2014**, *51*, 2116–2122. [[CrossRef](#)]
4. Le Calvez, J.; Malpini, R.; Xu, J.; Stokes, J.; Williams, M. Hydrolic fracturing insights from microseismic monitoring. *Oilfield Rev.* **2016**, *28*, 16–33.
5. Ishio, T.; Mizutani, H. Experimental and the theoretical basis of electrokinetic phenomena in rock-water systems and its application in gheophysics. *J. Geophys. Res.* **1981**, *86*, 1763–1775. [[CrossRef](#)]
6. Jaafar, M.Z.; Jackson, M.D.; Saunders, J.H.; Vinogradov, J.; Pain, C.C. *Measurements of Streaming Potential for Downhole Monitoring on Intelligent Wells*; SPE-120460-MS; Society of Petroleum Engineers: Houston, TX, USA, 2009.
7. Jackson, M.D.; Vinogradov, J.; Saunders, J.H.; Jaafar, M.Z. Laboratory measurements and numerical modeling of streaming potential for downhole monitoring in intelligent wells. *SPE J.* **2011**, *16*, 625–636. [[CrossRef](#)]
8. Saunders, J.H.; Jackson, M.D.; Pain, C.C. A new numerical model of electrokinetic potential response during hydrocarbon recovery. *Geophys. Res. Lett.* **2006**, *33*, 1–6. [[CrossRef](#)]
9. Eltsov, I.N.; Shelukhin, V.V.; Epov, M.I. Evolution of self-potential near the hole during drilling. *Dokl. Earth Sci.* **2011**, *436*, 241–245. [[CrossRef](#)]
10. Ghommem, M.; Qiu X.; Aidagulov, G.; Abbad, M. Streaming potential measurements for downhole monitoring of reservoir fluid flows: A laboratory study. *J. Petrol. Sci.* **2018**, *161*, 28–49. [[CrossRef](#)]
11. Shelukhin, V.V.; Eltsov, I.N. Geodynamics of the zone close to a borehole during drilling. *Dokl. Earth Sci.* **2012**, *443*, 537–542. [[CrossRef](#)]
12. Biot, M.A. Theory of elasticity and consolidation for a porous anisotropic solid. *J. Appl. Phys.* **1955**, *26*, 182–185. [[CrossRef](#)]
13. Amirat, Y.; Shelukhin, V.V. Homogenization of electroosmotic flow equations in porous media. *J. Math. Anal. Appl.* **2008**, *342*, 1227–1245. [[CrossRef](#)]
14. Hartsen, M.W.; Pride, S.R. Electrostatic waves from point sources in layered media. *J. Geophys. Res.* **1997**, *102*, 24745–24769. [[CrossRef](#)]
15. Wurmstich, B.; Morgan, F.D. Modeling of streaming potential responses caused by oil pumping. *Geophysics* **1994**, *59*, 46–56. [[CrossRef](#)]
16. Shelukhin, V.; Eltsov, I.; Paranichev, I. The electrokinetic cross-coupling coefficient: Homogenization approach. *World J. Mech.* **2011**, *1*, 127–136. [[CrossRef](#)]
17. Shelukhin, V.V.; Terentev, S.A. Frequency dispersion of dielectric permittivity and electric conductivity of rocks via two-scale homogenization of the Maxwell equations. *Prog. Electromagn. Res. B* **2009**, *14*, 175–202. [[CrossRef](#)]

18. Shelukhin, V.V.; Terentev, S.A. Homogenization of Maxwell equations and the Maxwell-Wagner dispersion. *Dokl. Earth Sci.* **2009**, *424*, 155–159. [[CrossRef](#)]
19. Shelukhin, V.V. Invasion around a horizontal wellbore. *Eur. J. Appl. Math.* **2008**, *19*, 41–60. [[CrossRef](#)]
20. Shelukhin, V.V.; Eltsov I.N. Dynamics of near borehole zone while drilling poroelastic layer. *Geophys. J.* **2012**, *34*, 265–272.



© 2019 by the authors. Licensee MDPI, Basel, Switzerland. This article is an open access article distributed under the terms and conditions of the Creative Commons Attribution (CC BY) license (<http://creativecommons.org/licenses/by/4.0/>).